Interference between independent fluctuating condensates

Anatoli Polkovnikov*‡§, Ehud Altman*¶, and Eugene Demler*

*Department of Physics, Harvard University, Cambridge, MA 02138; ‡Department of Physics, Boston University, Boston, MA 02215; and ¶Department of Condensed Matter Physics, The Weizmann Institute of Science, Rehovot 76100, Israel

Edited by Paul C. Martin, Harvard University, Cambridge, MA, and approved January 31, 2006 (received for review December 2, 2005)

We consider a problem of interference between two independent condensates that lack true long-range order. We show that their interference pattern contains information about correlation functions within each condensate. As an example, we analyze the interference between a pair of one-dimensional interacting Bose liquids. We find universal scaling of the average fringe contrast with system size and temperature that depends only on the Luttinger parameter. Moreover, the full distribution of the fringe contrast, which is also equivalent to the full counting statistics of the interfering atoms, changes with interaction strength and lends information on high-order correlation functions. We also demonstrate that the interference between two-dimensional condensates at finite temperature can be used as a direct probe of the Kosterlitz–Thouless transition. Finally, we discuss the generalization of our results to describe the interference of a periodic array of independent fluctuating condensates.

cold atoms | correlation functions | Luttinger liquids

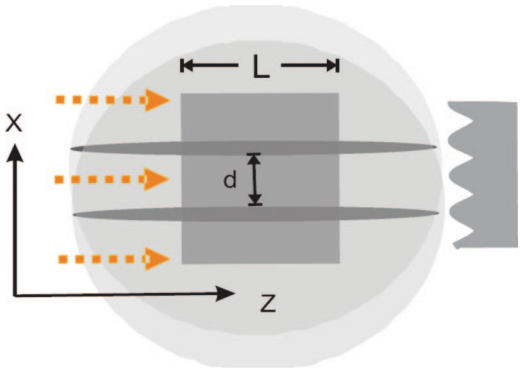

Fig. 1. Schematic view of the possible experimental setup, which produces an interference pattern between two independent one-dimensional condensates. Here, L and d are the imaging length and the separation between the condensates, respectively.

An important property of Bose–Einstein condensates is the existence of a coherent macroscopic phase. Thus, a crucial benchmark in the study of such systems was the observation of interference fringes when two independent condensates were allowed to expand and overlap (1). This "two-slit" experiment was carried out with cold atoms in three-dimensional harmonic traps, where a true condensate exists. The interference fringe amplitude should then be proportional to the condensate fraction, as was indeed observed. However, with current trapping technology it is possible to confine the bosonic atoms to one (2–4) or two dimensions (5), where a true condensate may not exist. Instead, these systems are characterized by off-diagonal correlations that either decay as a power-law or decay exponentially in space. What is the interference pattern that arises when two such imperfect condensates are allowed to expand and overlap? This question is not just of general academic interest. Recently there have been a number of experiments showing the interference between independent condensates (see, for example, refs. 6–8).

Here we address this problem theoretically and show that the result depends crucially on the correlations within each condensate. Therefore, such an experiment would provide a direct and simple probe of the spatial phase correlations. In principle, spatial phase correlations may also be extracted from juggling experiments (9–11) or the momentum distribution measured by the free expansion of a single condensate (2). However, creating strongly interacting low-dimensional systems typically requires using low-density atomic gases, which makes juggling experiments very challenging. In addition, the highly anisotropic expansion of low-dimensional condensates inhibit measurements of the momentum distribution in the slowly expanding longitudinal direction. A method for probing the phase correlations directly in real space would therefore be very useful.

Results

The simplest geometry that we consider is illustrated in Fig. 1 and consists of two parallel one-dimensional condensates a distance, d, apart. After the atoms are released from the trap, they are allowed to expand to a transverse size much larger than d, although no significant expansion occurs in the axial direction. An absorption image is then taken by a probe beam directed along the condensate axis. A similar setup is considered for two-dimensional condensates on parallel planes (see Fig. 2). As usual, the absorption image gives the instantaneous three-dimensional density profile integrated along the beam axis. $\rho(x) = \int_0^L dz\, a^\dagger_{\rm tof}(x,z)\, a_{\rm tof}(x,z)$, where $a^\dagger_{\rm tof}$ are the Bose creation operators with the subscript "time of flight" (tof), emphasizing that the corresponding operators are taken after free expansion of atoms, z is the axial coordinate and x is the coordinate along the detector (see Fig. 1). The length L is typically given by the focal length of the imaging beam. It may also be controlled more precisely by applying magnetic field gradients so that only a specified section of the cloud is resonant with the probe light. In principle, one can consider an experiment with a probe beam orthogonal to the plane containing two parallel one-dimensional condensates. In this case, it is possible to integrate the resulting interference image within an arbitrary interval and obtain dependence of the interference contrast on L (note that this dependence characterizes a single run and a series of experiments is still needed to find the average contrast). The other advantage of this setup is that it can reveal the presence of dipolar oscillations in individual condensates. These modes correspond to the center of mass motion and are not affected by interactions. Dipolar oscillations induce an overall tilt in the interference peak position and can be easily removed by integrating $\rho(x)$ along a line tilted with respect to the z axis. However,

Conflict of interest statement: No conflicts declared.

This paper was submitted directly (Track II) to the PNAS office.

Abbreviation: KT, Kosterlitz–Thouless.

§To whom correspondence should be addressed. E-mail: asp@bu.edu.

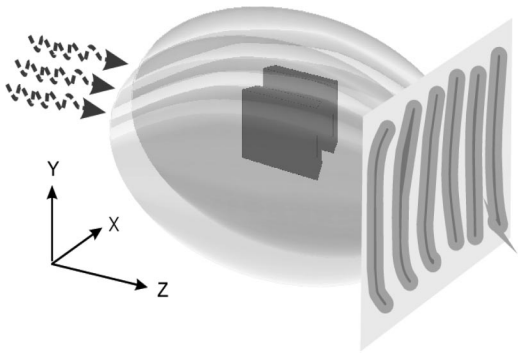

Fig. 2. Same as shown in Fig. 1, but this schematic is for two-dimensional condensates.

because most of the current experimental systems do not allow imaging beams that are perpendicular to one-dimensional condensates, we concentrate on the setup shown in Fig. 1.

To discuss the interference contrast, we consider the correlation function of the density operator,

$$\langle \rho(x_1)\rho(x_2)\rangle = \delta(x_1 - x_2)\int_0^L dz\rho(z) + \int_0^L dz_1 dz_2 \langle a^\dagger_{\rm tof}(r_1)a^\dagger_{\rm tof}(r_2)a_{\rm tof}(r_1)a_{\rm tof}(r_2)\rangle, \quad [1]$$

where r_i stands for (x_i, z_i). Single-particle operators in Eq. **1** should be taken after the expansion time t. We can relate them to operators before the expansion (12): $a_{\rm tof}(x, z) = a_1(z)e^{iQ_1(x)x - iQ_1^2 t/2m} + a_2(z)e^{iQ_2(x)x - iQ_1^2 t/2m}$, with a_1 and a_2 being operators in the two condensates and Q_1 and $Q_2 = m(x \pm d/2)/\hbar t$. We therefore find that the correlation function in Eq. **1** has an oscillating component at wave vector $Q = md/\hbar t$.

$$\langle \rho(x_1)\rho(x_2)\rangle_{\rm int} = \langle |A_Q|^2\rangle [e^{iQ(x_1 - x_2)} + c.c.], \quad [2]$$

$$\langle |A_Q|^2\rangle = \int_0^L dz_1 dz_2 \langle a^\dagger_2(z_1)a_1(z_1)a^\dagger_1(z_2)a_2(z_2)\rangle. \quad [3]$$

Here $A_Q = \int dz a^\dagger_1(z)a_2(z)$ is the quantum observable corresponding to the amplitude of the interference fringes. It can be extracted from the TOF absorption image by taking the Fourier transform of the density profile. Alternatively, one can directly probe A_Q^2 by studying the oscillating component in the density autocorrelation function. Both methods were successfully used in recent experiments (13, 14). In practice, it might be easier to study the interference contrast rather than the absolute value of the fringe amplitude. In this case, one has to divide A_Q by the imaging length L. If the two condensates are decoupled from each other, the expectation value of $\langle A_Q\rangle$ vanishes, which does not mean that $|A_Q|$ is zero in each individual measurement, but it does show that the phase of A_Q is random (15). Said differently, A_Q is finite in each experimental run, but its average over many experiments vanishes. To determine the amplitude of interference fringes in individual measurements, one should consider an expectation value of the quantity that does not involve the random phase of A_Q. This consideration naturally brings us to Eq. **3**. From shot to shot, $|A_Q|^2$ fluctuates as well, and Eq. **3** gives its average value.

If the two condensates are identical (but still independent), we may simplify Eq. **3**:

$$\langle |A_Q|^2\rangle = L\int_0^L dz \langle a^\dagger(z)a(0)\rangle^2. \quad [4]$$

Here, we neglected boundary effects by integrating over the center of mass coordinate and assuming that the correlations depend only on $(z_1 - z_2)$. Eq. **4** can be generalized for the case of parallel two-dimensional condensates by taking z to represent the planar coordinates.

To gain intuition into the physical meaning of the fringe amplitude, let us first address two simple limiting cases. First, consider the situation where $\langle a^\dagger(z)a(0)\rangle$ decays exponentially with distance with a correlation length $\xi \ll L$. Then, Eq. **4** implies that $|A_Q| \propto \sqrt{L\xi}$, which has a very simple physical meaning. Because the phase is only coherent over a length, ξ, the system is effectively equivalent to parallel chains with L/ξ pairs of independent condensates. Each pair contributes interference fringes with a constant amplitude proportional to ξ and a random phase. The total amplitude A_Q is therefore the result of adding L/ξ independent vectors of constant length ξ and random direction; hence, we get $\sqrt{L\xi}$ scaling. Note that the interference contrast, which is proportional to A_Q/L, the ratio of fringe amplitude to the background signal, scales as $\sqrt{\xi/L}$. This observation is similar in spirit to that made in ref. 6 of interference between 30 independent condensates in a chain. Fringes can be seen, although their average amplitude is suppressed by a factor of $\sqrt{30}$ compared with the interference between two condensates. Now consider the opposite limit of perfect condensates, for which $\langle a^\dagger(z)a(0)\rangle$ is constant. In this case, Eq. **4** implies that $|A_Q| \propto L$. Pictorially, this scaling is the result of adding vectors with a uniform phase, which results in a fringe amplitude that scales as the total size of the system, essentially the result of the experiment in ref. 1.

One-Dimensional Bose Liquids. We proceed to discuss the case of a one-dimensional interacting gas. We first consider a system at sufficiently low temperature, $\xi_T \gg L$, where ξ_T is the temperature-dependent correlation length defined in Eqs. **17** and **18**. In this regime, the correlations decay as a power-law rather than decay exponentially. We therefore, expect that the fringe amplitude will somehow interpolate between the two simple limits considered above. Specifically, at long wavelengths, the one-dimensional Bose gas is described by a Luttinger liquid (16), and the long-distance off-diagonal correlations behave as

$$\langle a^\dagger(z)a(0)\rangle \sim \rho\left(\frac{\xi_h}{z}\right)^{1/2K}. \quad [5]$$

Here, ρ is the particle density, ξ_h is the healing length, which also serves as the short-range cutoff, and K is the Luttinger parameter. For bosons with a repulsive short-range potential, K ranges between 1 and ∞, with $K = 1$ corresponding to strong interactions, or "impenetrable" bosons, and $K \to \infty$ corresponding to noninteracting bosons. Substituting Eq. **5** into Eq. **4** and assuming that $L \gg \xi_h$, we arrive at one of our main results:

$$\langle |A_Q|^2\rangle = C\rho^2 L^2\left(\frac{\xi_h}{L}\right)^{\frac{1}{K}}, \quad [6]$$

where C is a constant of order unity. Thus, we see that the amplitude of the interference fringes ($\bar{A}_{\rm O} \equiv \sqrt{\langle |A_Q|^2\rangle}$) scales with a nontrivial power of the imaging length. In the noninteracting limit ($K \to \infty$) the scaling is linear $\bar{A}_Q \sim$ L as expected for a fully coherent system. Interestingly $\bar{A}_Q \sim \sqrt{\rm L}$ in the hard-core

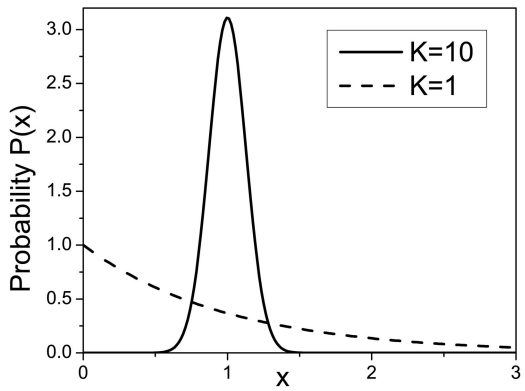

Fig. 3. Schematic plots of the distribution function $P(x)$ of the normalized intensity of interference fringes ($x = |A_Q|^2/\langle|A_Q|^2\rangle$) in strongly and weakly interacting regimes: $K \to 1$ and $K = 10$.

limit ($K = 1$), as in systems with short-range correlations, which were discussed above. A more-careful examination of the integral shows that, at $K = 1$, there are additional logarithmic corrections to the power-law scaling.

Having derived the amplitude of interference fringes, an interesting question is how this amplitude fluctuates from one experimental run to the next. To answer this question, one should consider higher moments of the operator $|A_Q|^2$. We find that all moments have the general form: $\langle|A_Q|^{2n}\rangle = \langle|A_Q|^2\rangle^n F_n(K)$. It follows that when $|A_Q|^2$ is normalized, its distribution function $P(|A_Q|^2/\langle|A_Q|^2\rangle)$ is fully determined by the Luttinger parameter, K. In particular, for large K values, the function $P(|A_Q|^2/\langle|A_Q|^2\rangle)$ becomes very narrow, characterized by the width $\sigma \equiv \sqrt{\langle|A_Q|^4\rangle - \langle|A_Q|^2\rangle^2}/\langle|A_Q|^2\rangle \approx \pi/(\sqrt{6}K)$. As expected, for $K \to \infty$, the width of the distribution goes to zero (17). In the opposite limit of $K \to 1$, the distribution takes another simple limiting form: $P(x) \approx e^{-x}$. It is interesting to point out that not only the scaling with L but also the whole distribution of the interference fringes at $K \to 1$ is equivalent to the one that arises in systems with short-range correlations. In Fig. 3, we schematically plot the two distributions obtained in the opposite limits of strong and weak interactions. Note that the true distribution at large K values is slightly asymmetric. We address this issue in ref. 18. We see that there is an interesting crossover from a narrow distribution in weakly interacting systems ($K \gg 1$) to a wide Poissonian distribution in the hard-core limit ($K \to 1$). In fact, one can show that there is a close connection between the distribution function $P(x)$ and the partition function of the boundary Sine–Gordon problem. This connection gives a direct link between interference of two one-dimensional quasicondensates and thermodynamics of a single impurity problem in a Luttinger liquid. Ref. 18 discusses the details of this problem and the crossover from weak to strong interactions.

We showed above that it is possible to extract K by analyzing the scaling of the fringe amplitude with system size or by analyzing its distribution at a given system size. Another approach involves changing the angle θ between the probe beam and the condensate axis while keeping the imaging length fixed. The resulting absorption image then corresponds to integration of the cloud density along a line at an angle θ to the z axis. Then Eq. **1** should be changed accordingly. Let $\bar{x}$ be the transverse coordinate on the screen ($z = 0$), then, in the second term in the right-hand side of Eq. **1**, we substitute $x = \bar{x} - z \tan\theta$. Then, we obtain the analogue of Eq. **4**:

$$\langle|A_Q|^2(\theta)\rangle = L\int_0^L dz\langle a^\dagger(z)a(0)\rangle^2\cos[q(\theta)z], \qquad [7]$$

where $q(\theta) = k_0 \tan\theta$. For sufficiently large imaging length ($qL \gg 1$), Eq. **7** yields

$$\langle|A_Q|^2(\theta)\rangle \sim (\rho^2 L\xi_h)(\xi_h q)^{1/K-1}. \qquad [8]$$

Thus, the Luttinger parameter may be extracted from the angle dependence of the fringe amplitude. For $qL \gg 1$ (i.e., very small angles), Eq. **7** reduces to Eq. **4**. Note that if one uses the imaging beam orthogonal to the condensates, then θ will simply be the angle between the z axis and the direction of integration of the interference contrast.

Before concluding this section, let us address the effect of temperature. It is well known that, at any finite temperature, the off-diagonal correlations in a one-dimensional Bose system must be short-ranged. Specifically, at sufficiently long distances, off-diagonal correlations decay exponentially with a correlation length $\xi_T \sim 1/T$. The zero-temperature results presented above are valid at sufficiently low temperature that $\xi_T \gg L$. At higher temperature such that $\xi_T \ll L$, the scaling of the fringe amplitude with length must be $|\bar{A}_Q| \sim \sqrt{L}$, as discussed above for systems with short-range correlations. However, as long as $\xi_T \gg \xi_h$, the temperature-dependence of the fringe amplitude is universal, and it depends only on the Luttinger parameter:

$$\langle|A_Q|^2 \sim L\rho^2\xi_h\left(\frac{\hbar^2}{m\xi^2}\frac{1}{T}\right)^{1-\frac{1}{K}}, \qquad [9]$$

This provides another experimental method to extract Luttinger physics.

Two-Dimensional Systems. We now consider a pair of parallel two-dimensional condensates. In direct analogy to the one-dimensional condensates, the imaging axis may be taken parallel or at some angle to the plane of the condensates. In the former case, one should consider the scaling of the fringe amplitude with imaging length, whereas, in the latter case, one should consider the variation with angle.

It is well known that in two dimensions long-range order may exist only at zero temperature. At sufficiently low temperatures, off-diagonal correlations are algebraic, with

$$\langle a^\dagger(\mathbf{r})a(\mathbf{0})\rangle \sim \rho\left(\frac{\xi_h}{r}\right)^\alpha, \qquad [10]$$

for $r \gg \xi_h$. In contrast, above the Kosterlitz–Thouless (KT) transition at $T = T_c$, the correlations decay exponentially. We will show that this transition is characterized by a jump in the behavior of the fringe amplitude, related to the well known universal jump of the superfluid stiffness at T_c.

The exponent in Eq. **10** is given by $\alpha = mT/2\pi\rho_s(T)\hbar^2$. For weakly interacting bosons at temperatures well below T_c, $\rho_s(T)$ is simply equal to the density, ρ. As one approaches the transition, ρ_s is renormalized by fluctuations, and, at the transition, $\rho_s(T_c) = 2mT_c/\pi\hbar^2$. Therefore, the exponent α assumes a universal value $\alpha_c = 1/4$ at the transition. Thus, for temperatures $T < T_c$, we have $0 < \alpha < \alpha_c$.

Let us now discuss the consequences of this physics to the experimentally measurable fringe amplitude. As illustrated in Fig. 1, the interference pattern is now truly two-dimensional in the sense that cuts along x at different coordinate, y, display a different fringe pattern. To obtain a one-dimensional pattern as a function of x alone, we may integrate the image intensity over an "integration length," L_y. Recall that, in addition, the imaging process automatically integrates over an imaging length L_z along the z axis. Now the generalization of Eq. **4** to the two-dimensional case is straightforward:

$$\langle |A_Q|^2 \rangle \sim L_y L_z \int_0^{L_y} dy \int_0^{L_z} dz \langle a^\dagger(y, z), a(0, 0) \rangle^2. \quad [11]$$

For simplicity, we assume that L_y and L_z are scaled simultaneously as $L_y = L_z = \sqrt{\Omega}$, with Ω being the imaging area. Then, with Eqs. **10** and **11**, we find that, for $T < T_c$,

$$\langle |A_Q|^2 \rangle \sim \Omega^{2-\alpha}. \quad [12]$$

So, below the transition, the scaling of $|A_Q|$ with size ranges from linear at $T = 0$ to $\Omega^{0.875}$ at the KT transition ($\alpha_c = 1/4$). In contrast, for $T > T_c$, the correlations decay exponentially and $|A_Q| \sim \sqrt{\Omega}$. Hence, we find a universal jump at $T = T_c$ in the power characterizing the size dependence of $|A_Q|$. One can also consider a setup for which only dependence on one length, say L_y, is studied, whereas the other one, L_z, is fixed. Then, if $L_y \gg L_z$, Eq. **12** immediately generalizes to $\langle |A_Q|^2 \sim L_y^{2-2\alpha}$. In this case, the power jump in $|A_Q|$ is bigger: from 0.75 to 0.5 as T crosses T_c. This jump is a direct signature of the KT physics to be contrasted with the result for one-dimensional condensates, for which the scaling power with system size interpolated smoothly between 1 and 2. It should be noted, however, that a one-dimensional system on an optical lattice, which undergoes a Mott transition at $T = 0$, would display a universal jump similar to the two-dimensional case discussed here. In the same way, one can study the shape of the distribution of the interference amplitude and find that, as T increases to T_c, the distribution gradually broadens but always remains relatively narrow. In contrast, as T becomes larger than T_c the distribution assumes a broad Poissonian form.

The analysis for imaging the two-dimensional condensates with a slanted probe beam can be carried over from the one-dimensional case. The scaling of the interference contrast with $q = k_0 \tan\theta$, at constant imaging area, is then $\langle |A_Q|^2 \rangle \sim 1/q^{2-2\alpha}$ below the KT transition, and $\langle |A_Q|^2 \rangle \sim 1/(1 + q^2\xi^2)^{3/2}$ above it. Again the transition is characterized by a universal jump of the power at small q. We emphasize that θ can be either the angle between the beam and the z axis (see Fig. 1) or the angle between the y axis and the direction of integration. The latter is preferable, because, within a single experimental shot, it is possible to obtain the whole angular dependence of $A_Q{}^2$.

Regardless of the experimental approach of choice, the interference between a parallel pair of independent two-dimensional condensates can serve as a direct probe of KT physics. However a word of caution is in order. The correlation length, which coincides with the healing length at very low temperatures (19) ($\xi_T \approx \xi_h = \hbar/\sqrt{mg\rho}$), diverges at the KT transition as $\xi_T \propto \exp(b/\sqrt{T_c - T}$ (20). Therefore, with increasing temperature, one has to probe the system at increasing distances $r \gg \xi_h(T)$ [or $L^{-1} \ll q \ll 1/\xi_h(T)$] to measure the asymptotic form of the correlation function given by Eq. **10**, which might hinder accurate determination of the universal jump.

Discussion

We considered a pair of interfering quasicondensates; however, most of our arguments can be generalized to the case of several independent condensates. Of particular interest is a periodic array of tubes (2–4) or pancakes created by an optical potential (5, 21, 22). The interference pattern in this case shows correlations at a set of wave vectors $Q_n = nQ$, where n is an integer and Q is determined by the distance between neighboring condensates. The size and angle dependence of the average interference amplitudes for each of these wave vectors should have the same scaling properties as two quasicondensates. However, the distribution function of fringe amplitudes will be different. In particular, in the limit of a large number of condensates, the distribution function should become very narrow. This result follows immediately from the observation that in this limit, higher-order correlation functions in TOF images are dominated by products of two point correlation function in different condensates, so there should be no broadening associated with Eq. **15** below.

Another point worth making regards the possibility of making analogous experiments with Fermions. For example, one can consider an interference of two independent one-dimensional fermionic systems. One obvious difference from the bosonic case will be the change of sign in the correlation function (see Eq. **2**), reflecting different statistics of the fermions (this corresponds to fermion antibunching). More importantly, the correlation function decays as $1/|x|^{1/2(K+1/K)}$, i.e., as $1/x$ or faster. This scaling means that the integral in Eq. **4** is dominated by short distances, at which the Luttinger liquid description is not sufficient, and that the integral converges as $L \to \infty$. Infrared convergence of Eq. **4** implies trivial scaling $|A_Q| \propto \sqrt{L}$. Moreover, the integrals appearing in all moments of the distribution are similarly infrared convergent, which results in a Poissonian fringe distribution at large L values: $P(x) \propto e^{-x}$, as found for bosons at high temperature. To extract information on the Luttinger parameter, one can analyze the decay of density–density correlations in the noise $\langle \rho_{\rm int}(x, z_0)\rho_{\rm int}(x, z_0 + z) \rangle$ as a function of z, which is directly related to the integrand of Eq. **4**. We note that these correlations have an oscillating component similar to Friedel oscillations, with wave vector $2k_f$. The oscillating component appears as a peak (cusp singularity) in the angular dependence of the interference contrast at an imaging angle $k_0 \tan\theta = 2k_f$ (see Eq. **7**). The shape of this cusp as well as of the cusp at $\theta = 0$ holds information on the Luttinger parameter. A more-detailed analysis of the fermionic case lies beyond the scope of this work.

In conclusion, we analyzed the interference between two independent quasicondensates. We showed that scaling properties of interference fringes directly probe the algebraic off-diagonal correlations. In particular, for one-dimensional condensates, the scaling with imaging length or with temperature allows the extraction of the Luttinger parameter. In the case of two-dimensional condensates, this method provides a unique probe of the KT transition. We also argued that, in the one-dimensional case, one can use the distribution function of the interference amplitude (which is also equivalent to the full counting statistics of interfering bosons) as the qualitative probe of the Luttinger constant. In particular, at $K \gg 1$ the distribution is narrow and at $K \to 1$ or, at finite temperatures, it becomes wide Poissonian (see Fig. 2). In the two-dimensional case, we expect a sharp change in the shape of the distribution function at the KT transition. The scaling analysis remains intact if more than two independent condensates are present, but the distribution functions can no longer be used as a probe of the correlations.

Methods

Luttinger Liquid Parameter. The Luttinger liquid provides a universal long-wavelength description of one-dimensional, interacting Bose liquids that allows the calculation of the long-distance behavior of correlations such as Eq. **5**. In certain regimes, it is possible to derive the Luttinger parameter, K, and the healing length, ξ_h, from the microscopic interactions. In particular, for bosons with weak contact interactions, relevant for ultra-cold atom systems discussed in this work, one can use Bogoliubov theory to obtain (23, 24)

$$\xi_h \approx \frac{1}{\rho\sqrt{\gamma}}, \qquad K \approx \frac{\pi}{\sqrt{\gamma}}\left(1 - \sqrt{\frac{\gamma}{2\pi}}\right)^{-1/2}. \quad [13]$$

.

Here, $\gamma \equiv 2/(a_{1d}\rho) \lesssim 1$ is a dimensionless measure of the interaction strength, and a_{1d} is the one-dimensional scattering

length. Analytic expressions for these parameters may also be derived in the limit of strong contact interaction $\gamma \gg 1$ (23):

$$\xi \approx 1/\rho, \qquad K \approx 1 + \frac{4}{\gamma}. \qquad [14]$$

Moments of the Fringe Amplitude. All of the moments in the distribution of $|A_Q|^2$ can be obtained by generalizing the two-point correlation function in Eq. **3** to the $2n$-point correlation function

$$\langle |A_Q|^{2n} \rangle = \int_0^L \dots \int_0^L dz_1 \dots dz_n dz'_1 \dots dz'_n$$
$$|\langle a^\dagger(z_1) \dots a^\dagger(z_n) a(z'_1) \dots a(z'_n) \rangle|^2. \qquad [15]$$

For bosons with repulsive interactions described by the Luttinger parameter, K, we have

$$\langle |A_Q|^{2n} \rangle = (\tilde{C}\rho^2 L^2)^n \left(\frac{\xi_h}{L}\right)^{\frac{n}{K}} \int_0^1 \dots \int_0^1 d\omega_1 \dots d\omega'_n$$
$$\left| \frac{\Pi_{i<j} |\omega_i - \omega_j| \Pi_{i<j} |\omega'_i - \omega'_j|}{\Pi_{ij} |\omega_i - \omega_j|} \right|^{1/K}, \qquad [16]$$

which is precisely of the form $\langle |A_Q|^{2n} \rangle = \langle |A_Q|^2 \rangle^n F_n(K)$. Integrals of the type appearing in Eq. **16** have been discussed by Fendley *et al.* (25), who demonstrated that they can be calculated by using special properties of Jack polynomials. From the knowledge of all moments, one can, in principle, construct the full distribution of the interference fringes amplitude. In this paper, we only discuss the limits of weak ($K \gg 1$) and strong ($K \approx 1$) interactions.

Finite Temperature Correlations in One Dimension. The finite-temperature, off-diagonal correlations are given by ref. 23:

$$\langle a^\dagger(z) a(0) \rangle \sim \rho \xi_h^{1/2K} \left(\frac{\pi/\xi_T}{\sinh \pi z/\xi_T} \right)^{1/2K}, \qquad [17]$$

where the thermal correlation length, ξ_T, is

$$\frac{\xi_T}{\xi_h} \approx \left(\frac{\hbar^2}{m\xi_h^2}\right)\frac{1}{T}. \qquad [18]$$

Eq. **17** is valid for sufficiently low temperatures so that $\xi_T \gg \xi_h$ or, equivalently, $T \ll \hbar^2/m\xi_h^2$. For $z \ll \xi_T$, Eq. **17** reduces to the zero temperature correlation (5). In the opposite limit, $z \gg \xi_T$, the correlation function given by Eq. **17** may be approximated by

$$\langle a^\dagger(z) a(0) \rangle \sim \rho \left(\frac{\xi_h}{\xi_T}\right)^{\frac{1}{2K}} e^{-\pi z/2K\xi_T}. \qquad [19]$$

As we already noted, for sufficiently low temperatures when $\xi_T > L$, the fringe amplitude may be found from Eq. **6**. For $L \gg \xi_T$, Eq. **19** implies

$$\langle |A_Q|^2 \rangle \sim L\rho^2 \xi_h^{1/K} \xi_T^{1-\frac{1}{K}}. \qquad [20]$$

Finally, substituting Eq. **18** for ξ_T gives Eq. **9**.

We also note that the angular dependence of the fringe amplitude at finite temperature is given by

$$\langle |A_Q|^2(\theta) \rangle \sim \rho^2 L \xi_h^{1/K} \xi_T^{1-\frac{1}{K}} \frac{K/\pi}{1 + K^2 q^2 \xi_T^2/\pi^2}. \qquad [21]$$

From this expression, it is harder to extract K directly because of uncertainty in the determination of ξ_h and, hence, ξ_T.

We thank P. Fendley, M. Greiner, V. Gritsev, Z. Hadzibabic, M. Lukin, M. Oberthaller, M. Oshikawa, J. Schmiedmayer, V. Vuletic, D. Weiss, and K. Yang for useful discussions. This work was supported in part by the U.S.–Israel Binational Science Foundation and by National Science Foundation Grant DMR-0132874.

1. Andrews, M. R., Townsend, C. G., Miesner, H. J., Durfee, D. S., Kurn, D. M. & Ketterle, W. (1997) *Science* **275,** 637–641.
2. Paredes, B., Widera, A., Murg, V., Mandel, O., Fölling, S., Cirac, I., Shlyapnikov, G. V., Hänsch, T. W. & Bloch, I. (2004) *Nature* **429,** 277–281.
3. Kinoshita, T., Wenger, T. R. & Weiss, D. S. (2004) *Science* **305,** 1125–1128.
4. Fertig, C. D., O'Hara, K. M., Huckans, J. H., Rolston, S. L., Phillips, W. D. & Porto, J. V. (2005) *Phys. Rev. Lett.* **94,** 120403.
5. Stock, S., Hadzibabic, Z., Battelier, B., Cheneau, M. & Dalibard, J. (2005) *Phys. Rev. Lett.* **95,** 190403.
6. Hadzibabic, Z., Stock, S., Battelier, B., Bretin, V. & Dalibard, J. (2004) *Phys. Rev. Lett.* **93,** 180403.
7. Schumm, T., Hofferberth, S., Andersson, L. M., Wildermuth, S., Groth, S., Bar-Joseph, I., Schmiedmayer, J. & Krüger, P. (2005) *Nat. Phys.* **1,** 57–62.
8. Shin, Y., Sanner, C., Jo, G.-B., Pasquini, T. A., Saba, M., Ketterle, W., Pritchard, D. E., Vengalattore, M. & Prentiss, M. (2005) *Phys. Rev. A* **72,** 021601.
9. Hagley, E. W., Deng, L., Kozuma, M., Wen, J., Helmerson, K., Rolston, S. L. & Phillips, W. D. (1999) *Science* **283,** 1706–1709.
10. Bloch, I., Hänsch, T. W. & Esslinger, T. (2000) *Nature* **403,** 166–170.
11. Petrov, D. S., Shlyapnikov, G. V. & Walraven, J. T. M. (2000) *Phys. Rev. Lett.* **85,** 3745–3749.
12. Roth, R. & Burnett, K. (2003) *Phys. Rev. A* **67,** 031602(R).
13. Greiner, M., Regal, C. A., Stewart, J. T. & Jin, D. S. (2005) *Phys. Rev. Lett.* **94,** 110401.
14. Foelling, S., Gerbier, F., Widera, A., Mandel, O., Gericke, T. & Bloch, I. (2005) *Nature* **434,** 481–484.
15. Castin, Y. & Dalibard, J. (1997) *Phys. Rev. A* **55,** 4330–4337.
16. Haldane, F. D. M. (1981) *Phys. Rev. Lett.* **47,** 1840–1843.
17. Javanainen, J. & Yoo, S. M. (1996) *Phys. Rev. Lett.* **76,** 161–165.
18. Gritsev, V., Altman, E., Demler, E. & Polkovnikov, A. (2006) arXiv: cond-mat/0602475.
19. Petrov, D. S., Holzmann, M. & Shlyapnikov, G. V. (2000) *Phys. Rev. Lett.* **84,** 2551–2555.
20. Chaikin, P. M. & Lubensky, T. C. (1995) *Principles of Condensed Matter Physics* (Cambridge Univ. Press, Cambridge, U.K.).
21. Eiermann, B., Treutlein, P., Anker, T., Albiez, M., Taglieber, M., Marzlin, K.-P. & Oberthaler, M. K. (2003) *Phys. Rev. Lett.* **91,** 060402.
22. Cataliotti, F. S., Burger, S., Fort, C., Maddaloni, P., Minardi, F., Trombettoni, A., Smerzi, A. & Inguscio, M. (2001) *Science* **293,** 843–846.
23. Cazalilla, M. A. (2004) *J. Phys. B* **37,** S1–S47.
24. Mora, C. & Castin, Y. (2003) *Phys. Rev. A* **67,** 053615.
25. Fendley, P., Lesage, F. & Saleur, H. (1995) *J. Stat. Phys.* **79,** 799–819.